Journal of Power Sources 243 (2013) 779–789

Contents lists available at SciVerse ScienceDirect

Journal of Power Sources

journal homepage: www.elsevier.com/locate/jpowsour

Simulation and evaluation of capacity recovery methods for spiral-wound lithium ion batteries

Yonghuang Ye [a], Yixiang Shi [b], Lip Huat Saw [a], Andrew A.O. Tay [a,*]

[a] Department of Mechanical Engineering, National University of Singapore, 9 Engineering Drive 1, Singapore 117576, Singapore
[b] Key Laboratory for Thermal Science and Power Engineering of Ministry of Education, Tsinghua University, Beijing 100084, China

HIGHLIGHTS

- An electrochemical model for evaluating different capacity recovery methods for cycled batteries.
- Center recovery method on commercial battery and novel battery with porous current collectors.
- Comparisons between center recovery method and bottom recovery method.
- Comparisons between recovery method by discharging negative electrodes and by discharging positive electrodes.

ARTICLE INFO

Article history:
Received 6 March 2013
Received in revised form
12 June 2013
Accepted 14 June 2013
Available online 22 June 2013

Keywords:
Lithium ion battery
Spiral-wound
Porous current collector
Capacity recovery

ABSTRACT

An electrochemical model is developed to investigate capacity recovery methods for cycled lithium ion batteries. Different capacity recovery methods are evaluated and compared. The center recovery method for commercial batteries is found to be impractical because it causes severe solid surface concentration gradients which may harm the batteries. On the contrary, the center recovery method for novel batteries with porous current collector sheets is better than the bottom recovery method because smaller solid surface concentration gradients are detected and less relaxation time is required during capacity recovery. Capacity recovery methods which discharge negative electrodes is superior to those which discharge positive electrodes of cycled batteries as smaller solid surface concentration gradients is generated and less relaxation time is required at the same discharging current.

1. Introduction

Lithium ion batteries have been targeted for use in the automotive and space industries that demand exceptionally long calendar and cycle lives [1]. However, lithium ion batteries still suffer from the problems of capacity loss and limited cycle life. The capacity fading of lithium ion batteries is caused by several different mechanisms associated with side reactions, leading to electrolyte decomposition, passive film formation, active material dissolution, and other phenomena [2,3]. In general, one of the most important reasons why batteries lose capacity and/or power capability is the loss of active lithium due to the formation of SEI (Solid Electrolyte Interface) layers [3–9]. When the amount of active lithium decreases during a battery's calendar and cycle life, the cell capacity decreases accordingly [1].

Much research has been done on extending the cycle life of batteries, and one novel method is to replenish the lost active lithium of cycled batteries. Wang et al. [1] proposed a method (bottom recovery method) for extending the life of a $LiFePO_4$/graphite lithium ion battery by replenishing the lost active lithium during cell operation and concomitant capacity fade. Active lithium was inserted into the battery by discharging the positive electrode (cycled battery with cap end removed) against a lithium metal electrode after the cycled battery has lost a significant amount of its capacity. About half of the lost capacity was recovered, and the cell was cycled for an additional 1500 cycles [1] before failure. Though the work shows promise for the in situ rejuvenation of a lithium ion battery, the replenishment employs a very low current due to the tightly-wound jelly roll design of the cylindrical cell. Further development in engineering design of the battery is necessary to significantly reduce the replenishment time to enable its use in practical systems [1].

Another capacity recovery method (center recovery method) which employs a lithium metal electrode inserted into the battery

* Corresponding author. Tel.: +65 65162207; fax: +65 67791459.
E-mail addresses: yeyonghuang1@163.com, A0086270@nus.edu.sg (Y. Ye), mpetayao@nus.edu.sg (A.A.O. Tay).

0378-7753/$ – see front matter © 2013 Elsevier B.V. All rights reserved.
http://dx.doi.org/10.1016/j.jpowsour.2013.06.083

Nomenclature

c	lithium ion concentration (mol m^{-3})
$_D$	lithium ion diffusivity (m^2 s^{-1})
E	cell potential (V)
F	Faraday constant (C mol^{-1})
i_0	exchange current density (A m^{-2})
j_{loc}	local current density (A m^{-2})
k_0	reaction rate constant (m$^{2.5}$ mol$^{-0.5}$ s^{-1})
r	radius distance variable of particle (m)
r_p	characteristic particle radius of electrode particles (μm)
S_a	specific surface area (m^{-1})
T	temperature (K)
t_+	transference number of Li ion species dissolved in liquid
U	thermodynamic, open circuit voltage (V)
v	thermodynamic factor relating to electrolyte activity
x	distance variable through a cell component (m)
y	dimensionless radial distance of particles

Greek letters

α_a	transfer coefficient for anodic current
α_c	transfer coefficient for cathodic current
ε_1	active material volume fraction
ε_2	volume fraction
ϕ	electric potential (V)
γ	Bruggeman tortuosity exponent
σ	electrical conductivity (S m^{-1})
η	over potential (V)

Subscripts, superscripts and acronyms

0	initial or equilibrated state
1	solid phase
2	liquid phase
ref	reference composition or relative to a Li/lithium ion reference electrode

was proposed in our previous study [10], although the feasibility of the method has not yet been verified. It is therefore interesting to evaluate the feasibility of this method using simulation and compare its performance with the bottom recovery method.

Considering that the replenishment current is limited by the tightly-wound jelly roll design of the cylindrical cell [1], and that the mass transfer in the liquid phase is restrained by the current collector foil, one may like to try using a porous current collector sheet which allows mass transfer across the current collector. Porous current collector sheets can be produced by either meshing [11] or sintering [12]. The major difference between a porous current collector sheet and a normal current collector foil is that the mesh structure or porous structure offers channels for electrolyte transfer and charge transfer across the current collector. A porous current collector is expected to help increase the recovery current density and reduce the replenishing time. Simulations, rather than experimental testing, are done to verify this idea as no cylindrical lithium ion battery with porous current collector sheets is commercially available yet.

In this study, the center recovery method and the bottom recovery method were simulated for both a commercial battery with normal current collector foils and a novel battery with porous current collector sheets. Comparisons are made on the performance of the two different recovery methods for different batteries on the basis of SOC (State of Charge, actual lithium ion concentration over maximum lithium ion concentration) evolution, SOC distribution, and discharging potential.

2. Model development

2.1. Center recovery by inserting lithium metal electrode into the center of the battery

2.1.1. Commercial lithium ion battery with normal current collector foil

The objective of the simulation is to verify the feasibility of the battery capacity recovery method proposed in our previous study [10]. In this method, a lithium metal rod is inserted into a cycled battery with its cap end removed, The lithium metal electrode is immersed in the electrolyte and acts as a source of lithium ion for replenishing the battery electrodes.

An electrochemical model for a commercial spiral-wound cylindrical 26650 (26 mm diameter, and 65 mm height) lithium ion battery (Fig. 1(b)) was developed following Ye et al. [10] and Somasundaram et al. [13]. The calculation domain is simplified to be two dimensional (2D), which is along the cross-section (A–A) of the battery, Fig. 1(b). Fig. 1(a) shows the schematic of the spiral-wound battery. The number of windings of the battery is 32 for the 26650 cylindrical battery. Each functional layer of the spiral-wound battery (including positive electrodes (pe), negative electrodes (ne), current collectors (cc), and separators (sp) were presented in different calculation domains. Current collectors are sandwiched in between two identical porous electrodes, and there are separators between the sandwich structure of positive electrodes and negative electrodes. Boundaries of the multi-layer structure are labeled B1 to B8.

A lithium metal domain is at the center of the battery, and electrochemical kinetics, see Eqs. (1)–(3), of the lithium metal electrode is applied on the interface B0 between the lithium metal domain and the electrolyte domain, as shown in Fig. 1:

$$i_2 = \sigma_2^{\text{eff}}\left[-\nabla\phi_2 + \frac{2RT}{F}\left[1+\frac{\partial \ln f}{\partial \ln c_2}\right](1-t_+)\frac{\nabla c_2}{c_2}\right] = j_{\text{loc}} \quad (1)$$

$$j_{\text{loc}} = i_0\left(\exp\left(\frac{\alpha_a F\eta}{RT}\right) - \exp\left(\frac{-\alpha_c F\eta}{RT}\right)\right) \quad (2)$$

$$\eta = \phi_1 - \phi_2 - U_{\text{ref,lithium}} \quad (3)$$

where j_{loc} is the local current density, i_0 is the exchange current density (of magnitude 12.6 A m^{-2} [14]), η is the over potential, φ_1 is the potential of the solid surface (lithium metal), φ_2 is the liquid phase potential, $U_{ref,\ lithium}$ is the equilibrium potential of lithium metal, which is set to zero in the model.

Governing equations and boundary conditions (electronic charge, ionic charge and mass balance) for the calculation domains of the spiral-wound geometry are listed in Tables 1 and 2, respectively.

The capacity recovery is realized either by discharging the positive electrode or the negative electrode of the battery against the lithium metal electrode. In the simulation, a uniform current source is applied on the positive current collector or the negative current collector. In the spiral-wound geometry, the current is considered to be entering the battery as a bulk source in the positive current collector. The effect of current collector tabs, which was

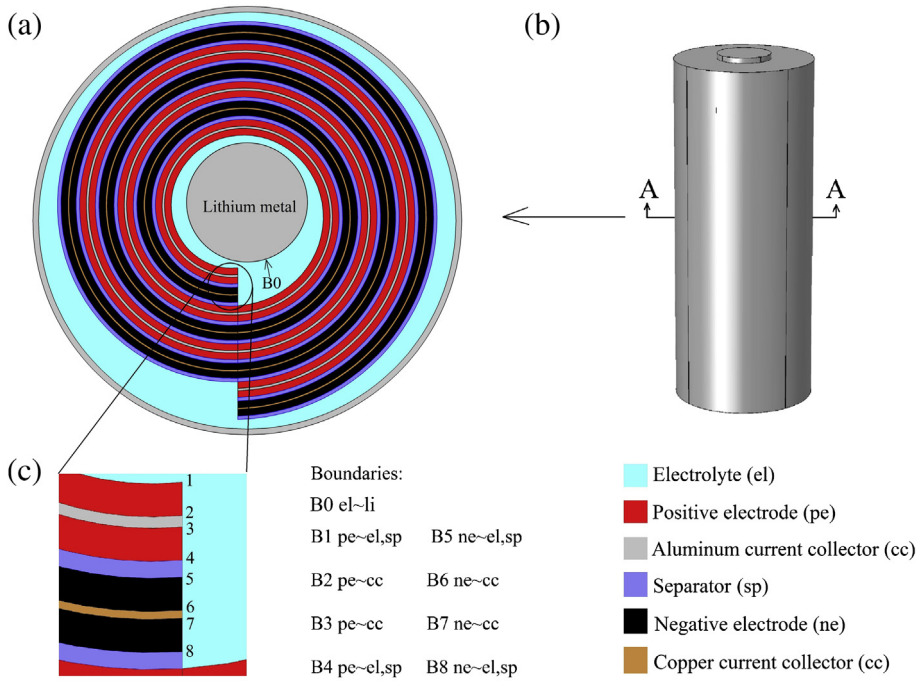

Fig. 1. Schematics of the calculation domains for the battery capacity recovery model, (a) calculation domains; (b) battery; (c) boundaries.

neglected in the work of Somasundaram et al. [13], is also neglected in this study (there are 4 current collector tabs for each current collector foil).

2.1.2. Spiral lithium ion battery with porous current collector sheet

A porous current collector sheet can be produced either by meshing [11] or by sintering [12]. The major difference between porous current collector sheet and normal current collector foil is that the mesh structure or porous structure offers channels for electrolyte transfer and charge transfer across the current collector.

The electrochemical model for a battery with normal current collector foils has been presented in Table 1, while in the case of a novel battery with porous current collector sheets, due to the porous structure of the current collectors, Eqs. (5) and (7) are employed on the current collectors for the charge and mass balances through the pores. The boundary conditions at the interfaces between porous electrodes and current collectors (B2, B3, B6, B7) for ionic charge is changed from "insulated" to "continuity' and mass balances is changed from "impermeable" to "permeable" in Table 2. Standard Bruggemann corrections [15] for tortuosity are employed for the correction of conductivity and diffusivity of electrolyte as well as the conductivity of the current collectors, as shown in Eqs. (9)–(11), respectively. These corrections are the same as those we have employed on the porous electrodes because of their similar porous structure.

$$\sigma_2^{\text{eff}} = \sigma_2 \varepsilon_2^{\gamma_2} \tag{9}$$

Table .1
Governing equations of electrochemical model for spiral-wound lithium ion battery.

Mechanisms	Equations		Correlations
Charge balance			
Solid phase (pe, ne, cc)	$\nabla\cdot\left(-\sigma_1^{eff}\nabla\phi_1\right) = -S_a j_{\text{loc}}$	(4)	$S_a = \frac{3\varepsilon_1}{r_p}$; $\sigma_1^{eff} = \sigma_1\varepsilon_1^{\gamma_1}$
			$E = \phi_1\vert_{B2} - \phi_1\vert_{B7}$
Solution phase (pe, ne, sp, el)	$\nabla\cdot\left\{\sigma_2^{eff}\left[-\nabla\phi_2 + \kappa_{junc}\frac{\nabla c_2}{c_2}\right]\right\} = S_a j_{\text{loc}}$	(5)	$\sigma_2^{\text{eff}} = \sigma_2\varepsilon_2^{\gamma_2}$
			$\kappa_{\text{junc}} = \frac{2RT}{F}\left[1+\frac{\partial \ln f}{\partial \ln c_2}\right](1-t_+) = \frac{2RT}{F}\nu$
Mass balance			
Solid phase (pe, ne)	$\frac{dc_1}{dt} + \frac{\partial}{\partial r^2}\left(-r^2 D_1 \frac{\partial}{\partial r}(c_1)\right) = 0$	(6)	$\frac{\partial c_1}{\partial r}\vert_{r=0} = 0$; $-D_1\frac{\partial c_1}{\partial r}\vert_{r=r_p} = \frac{j_{\text{loc}}}{S_a F}$
Solution phase (pe, ne, sp, el)	$\varepsilon_2\frac{dc_2}{dt} + \nabla\cdot\left\{-D_2^{\text{eff}}\nabla c_2\right\} = \frac{S_a j_{\text{loc}}}{F}(1-t_+)$	(7)	$D_2^{\text{eff}} = D_2\varepsilon_2^{\gamma_2}$
Electrochemical kinetics			
Bulter–Volmer equation (pe, ne)	$j_{\text{loc}} = i_0\left\{\exp\left(\frac{\alpha_a\eta F}{RT}\right) - \exp\left(\frac{-\alpha_c\eta F}{RT}\right)\right\}$	(8)	$\eta = \phi_1 - \phi_2 - U_{\text{ref}}$
			$i_0 = Fk_0 c_2^{\alpha_c}(c_{1,\max} - c_{1,\text{surf}})^{\alpha_c} c_{1,\text{surf}}^{\alpha_a}$

Table .2
Boundary conditions for electronic charge, ionic charge and mass balance.

Boundary	Electronic charge, ϕ_1	Ionic charge, ϕ_2	Mass balance, c_2
B0	0 V	Insulated	Impermeable
B1	Insulated	Continuity	Continuity
B2	Continuity	Insulated	Impermeable
B3	Continuity	Insulated	Impermeable
B4	Insulated	Continuity	Continuity
B5	Insulated	Continuity	Continuity
B6	Continuity	Insulated	Impermeable
B7	Continuity	Insulated	Impermeable
B8	Insulated	Continuity	Continuity

$$D_2^{\text{eff}} = D_2 \varepsilon_2^{\gamma_2} \tag{10}$$

$$\sigma_1^{\text{eff}} = \sigma_1 \varepsilon_1^{\gamma_1} \tag{11}$$

2.2. Bottom recovery method with battery cap end removed

The battery capacity recovery method proposed by Wang et al. [1] is to discharge the positive electrode against an external lithium metal electrode with the battery cap end removed as shown in Fig. 2(a), and this method is therefore called the bottom recovery method in this paper. In the simulation, the lithium ion battery is simplified as a 2D geometry with points A and B corresponding to the top end of battery, and points C and D corresponding to the bottom end of the battery. A piece of lithium metal immersed in the electrolyte is used to provide active lithium to one of the two electrodes during replenishment.

The governing equations and boundary conditions for this model are the same as those of capacity recovery for commercial lithium ion battery with normal current collector foils, Eqs. (4)–(8), as shown in Table 2. Electrochemical kinetics for the lithium metal electrode is applied on the interface between the lithium metal electrode and the electrolyte (Eqs. (1)–(3)).

It is straightforward to see from Fig. 2(b) that the current collector does not affect the discharging process of the positive electrode or the negative electrode, that is, the introduction of porous current collector sheets makes no difference in the bottom recovery method. In the bottom recovery method, lithium ions are transported along the vertical direction (from bottom to top of the battery), while the channels provided by the porous structure of the porous current collector sheets do not improve the transport performance of lithium ions. In this study, simulations were done for the bottom recovery method both on a commercial battery and a novel battery. Since the results are the same, the simulation results for the bottom recovery method on the novel battery are not presented here.

2.3. Model parameters

Since the electrochemical model is developed for the same type of lithium ion battery (26650 cylindrical $LiFePO_4$ battery) in our previous work [10] and the works of Wang et al. [1,16], the model parameters are identical to those presented in our previous lumped electro–thermal cycle life model [10]. For the sake of simplicity, model parameters are not shown again here, one can refer to Ref. [10] for details.

In the electrochemical model for spiral-wound lithium ion battery with porous current collectors, the porosity of the current collectors are assumed to be 0.54, that is $\varepsilon_1 = \varepsilon_2 = 0.54$. Though there is no data available for commercial porous current collectors, we took this value from the experimental data from Xu et al. [12].

3. Case study

In this study, the same case in the experimental test by Wang et al. [1] is simulated. In the experiment of Wang et al., the commercially available 2.2 Ah, 26,650 cylindrical cells (A123System Inc.) were cycled using Arbin BT-2400 system at 45 °C to introduce capacity fade. During each cycle, the cell was charged to a maximum voltage of 3.6 V at C/2 rate followed by constant current charging until the current was less than 0.1 A, A capacity of 1.6 Ah at a rate of C/2 was used for the discharge cycle. The End-of-Life of the cycled battery was defined as when the battery has lost 30% of its initial capacity [1]. The battery was opened at the bottom and immersed into an electrolyte solution of 1 M $LiPF_6$ in EC/DMC (1:1). The positive electrode of the cycled battery was discharged against the lithium metal electrode with a constant current of 0.5 mA while the graphite anode was idling. The positive electrode is kept

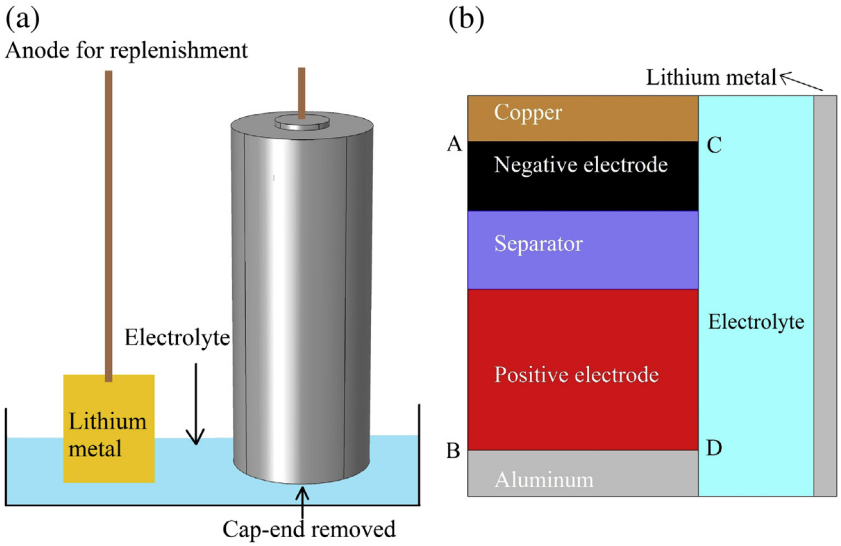

Fig. 2. Schematic of battery capacity recovery model, bottom recovery with cap end removed, (a) schematic of set up; (b) schematic of calculation domains.

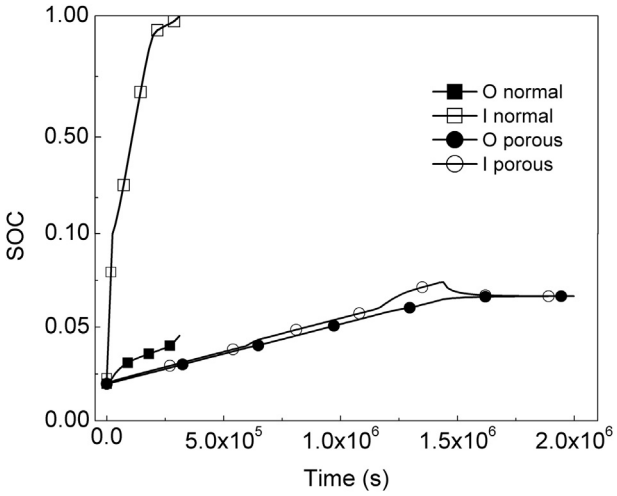

Fig. 3. Comparison of solid surface SOC evolution during capacity recovery between center recovery for commercial battery and novel battery.

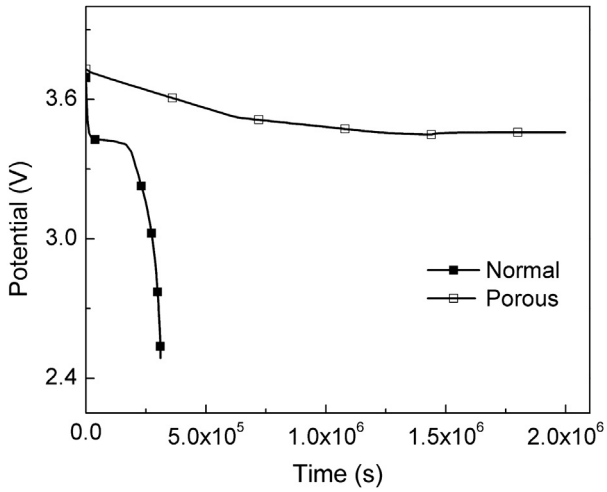

Fig. 5. Comparison of potential during capacity recovery between center recovery for commercial battery and novel battery.

discharged until the discharged capacity reaches 200 mAh, the battery is then set at rest for 24 h to allow for lithium ion diffusion within the cell [1]. Different cases are simulated as follows.

3.1. Center recovery for commercial battery with normal current collector foils

The center recovery method proposed in our previous study is a conceptual design, and it is of great interest to evaluate the feasibility of this method. In the simulation, the positive electrode of the cycled battery is discharged against a lithium metal electrode inserted into the battery center with 0.5 mA current supply. The discharging potential, liquid phase concentration, and liquid phase potential during the capacity recovery process will be simulated and evaluated so as to verify the feasibility of this center recovery method.

3.2. Center recovery for novel battery with porous current collector sheets

As mentioned in the introduction section, a novel battery with porous current collector sheets allows the liquid phase conduction and diffusion across the current collectors because of the porous structure of the porous current collector sheets, it is interesting to investigate whether the novel battery performs better in the capacity recovery process. In this attempt, capacity recovery applying 0.5 mA discharging current on the positive electrode of the novel battery is performed to compare with the recovery performance on the commercial battery. After that, the recovery current is increased to 5 mA and 50 mA to further evaluate the performance of center recovery method on the novel battery with porous current collector sheets.

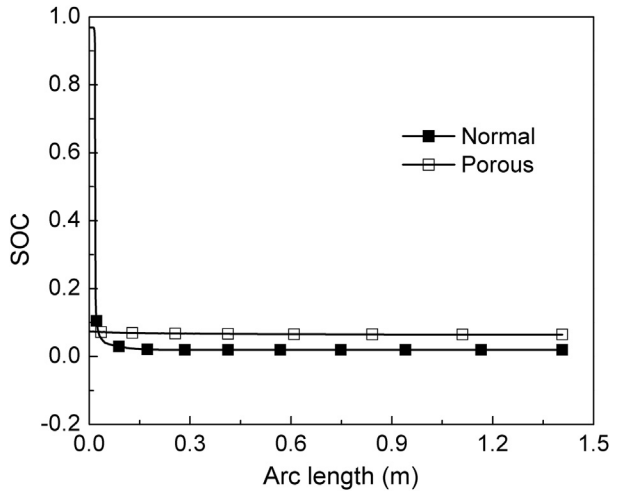

Fig. 4. Comparison of solid surface concentration distribution during capacity recovery between center recovery for commercial battery and novel battery (O for outer terminal, I for inner terminal).

3.3. Bottom recovery for commercial battery and novel battery

The bottom recovery method proposed by Wang et al. [1] discharges the positive electrode of a cycled battery against a lithium metal electrode with 0.5 mA current, which is quite small and requires a long time (400 h for 200 mAh capacity recovery) for the recovery process. In this simulation, we would like to see if the bottom recovery method can employ higher recovery currents so as to reduce the recovery time required. The recovery current is increased to 5 mA and 50 mA, and similar to the previous simulation, the discharging potential, liquid phase concentration and solid surface concentration will be evaluated.

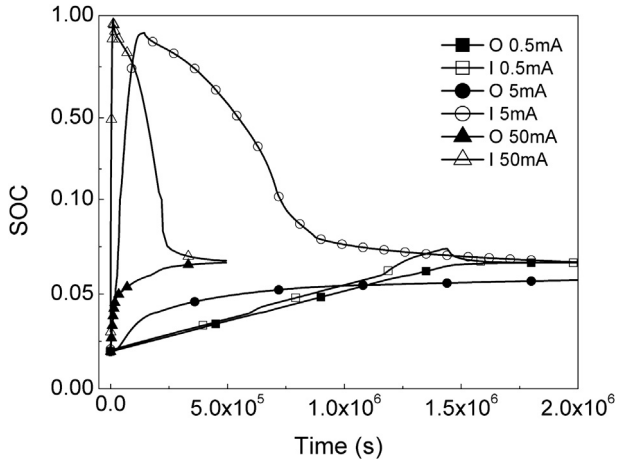

Fig. 6. Solid surface concentration evolution for center recovery of novel battery with varying recovery current.

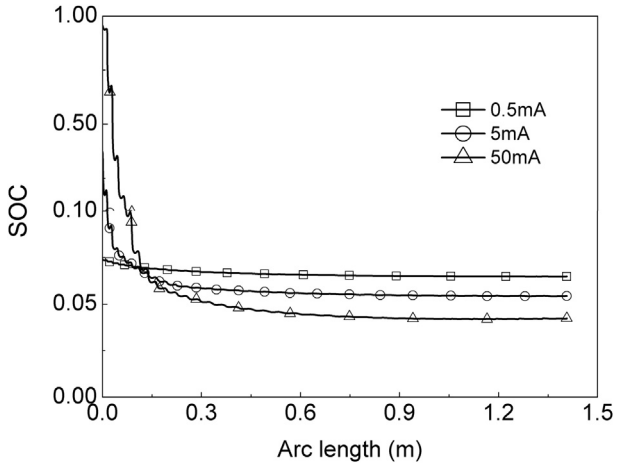

Fig. 7. SOC distribution for center recovery of novel battery with varying recovery current.

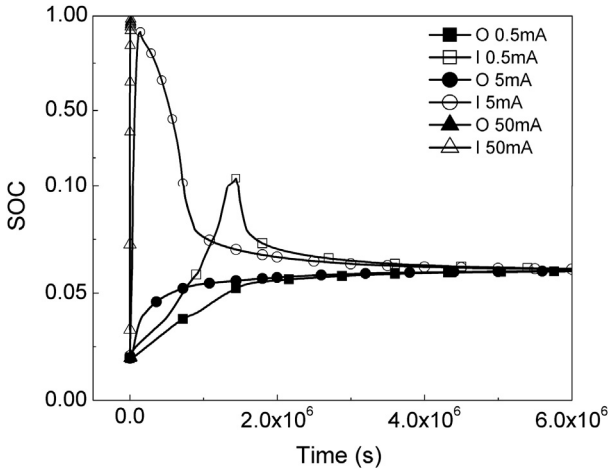

Fig. 9. Solid surface concentration evolution for bottom recovery with different recovery current.

3.4. Center recovery and bottom recovery by discharging the negative electrode

Similar recovery processes can be performed on the negative electrode by discharging the negative electrode against a lithium metal electrode so as to replenish the active lithium into the cycled battery. Different discharging currents varying from 0.5 mA to 50 mA are applied on the negative electrode in both center recovery method and bottom recovery method so as to compare with those of recovery method involving discharging of the positive electrodes.

4. Results and discussion

4.1. Comparison of center recovery on commercial battery and novel battery

The simulation results of solid surface SOC evolution, solid surface SOC distribution at the end of discharging and the discharging potential are shown in Figs. 3–5, respectively. The solid surface concentration at the terminal points of boundary B2 in the process of capacity recovery for a commercial battery with normal current collector shows that the solid surface concentration reaches the maximum value (corresponding to SOC = 1), and severe concentration gradient is found near the innermost terminal point as shown in Fig. 4. The discharging potential drops sharply before the recovered capacity reaches 50 mAh, far less than the targeted 200 mAh. A discharging current of 0.5 mA is too small for a practical recovery process, as the corresponding recovery time for a capacity of 200 mA is 400 h which is unacceptable. It is impractical to further lower the discharging current to mitigate the concentration inhomogeneity.

Fortunately, it is great to see much better recovery performance on the novel battery with porous current collector sheets. In the case for the novel battery with porous current collector sheets, with a discharging current of 0.5 mA, a much lower maximum concentration (SOC of 0.07 as compared to 1) and better concentration uniformity are detected. The discharging potential experiences a moderate drop in the recovery process as shown in Fig. 5. We may draw the conclusion that center recovery for commercial batteries with normal current collector foils is impractical, while it is promising to apply the center recovery method on novel batteries with porous current collector sheets.

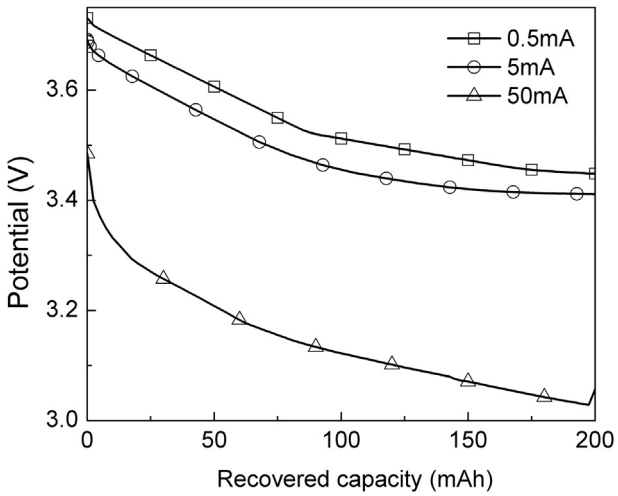

Fig. 8. Potential evolution for center recovery of novel battery with different recovery current.

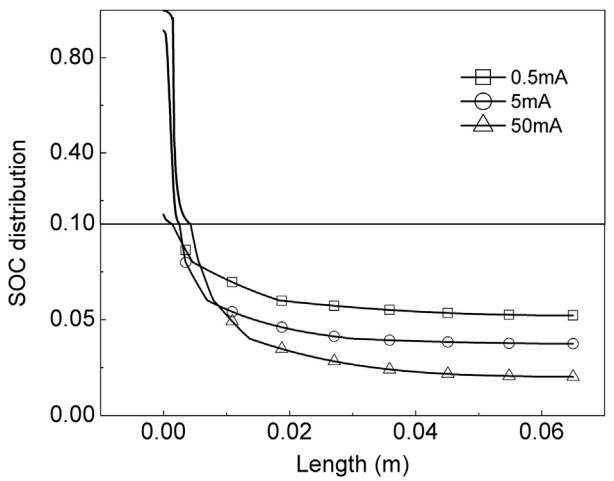

Fig. 10. Solid surface concentration distribution for bottom recovery with varying recovery current.

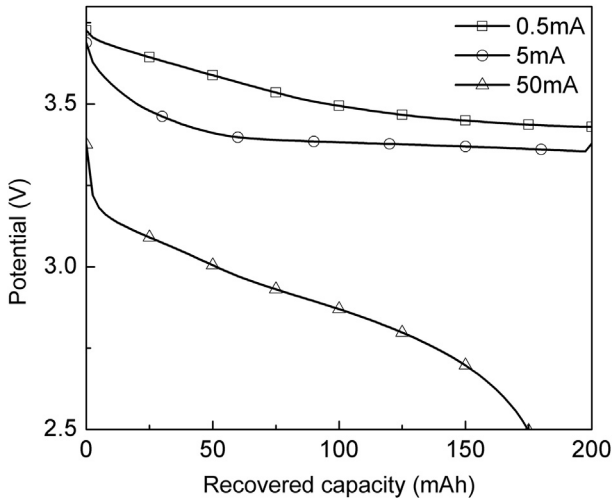

Fig. 11. Potential evolution for bottom recovery with varying recovery current.

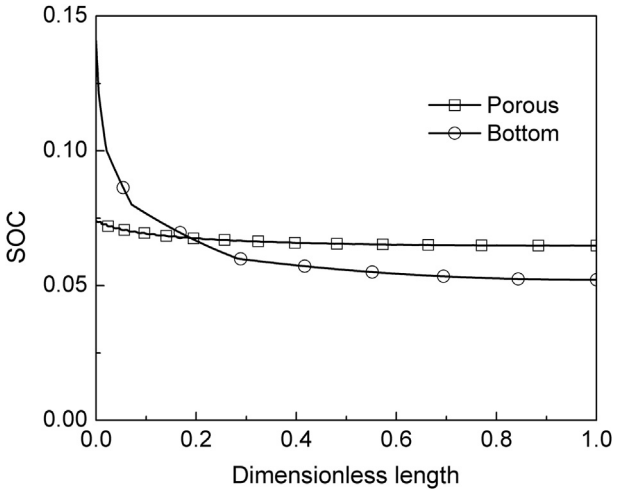

Fig. 13. Comparison of solid surface concentration distribution between bottom recovery and center recovery for novel battery with porous current collectors.

4.2. Center recovery on novel battery with varying discharging current

As discussed previously, the time for recovering 200 mAh capacity into the battery is 400 h when using a 0.5 mA discharging current. One may be interested in reducing the recovery time by applying higher discharging currents. In the simulation, the discharging current is varied from 0.5 mA, to 5 mA and 50 mA. Once again, the solid surface concentration evolution, solid surface concentration distribution and the discharging potential are analyzed.

As shown in Figs. 6 and 7, it is apparent that a 0.5 mA discharging current generates the smallest solid concentration gradient along boundary B2, and the maximum SOC is around 0.07, while the maximum SOC for 5 mA and 50 mA discharging currents almost reach the upper limit of SOC = 1. The discharging potential experiences a significant drop with a 50 mA discharging current as shown in Fig. 8. The total recovery time should be considered as the sum of discharging time and relaxation time. The relaxation time is the period required for the battery to reach an equilibrium state after discharging. The recovery time is 1.6×10^6 s for a 0.5 mA discharging current, and more than 2.0×10^6 for a 5 mA discharging current. However, the recovery time for a 50 mA discharging current is unexpectedly 5.0×10^5 s which is significantly shorter than the above two. It should be noted that a high discharging current can lead to extremely high maximum solid surface concentration (Fig. 6) and severe solid surface concentration gradient (Fig. 7). Thus a high discharging current may be detrimental to the battery and is unfavorable for the recovery process. It can also be seen from Fig. 7 that a higher discharging rate will cause greater SOC inhomogeneity but does not necessarily increase the relaxation time. Moreover, a discharging current corresponding to the minimum recovery time is not always the best choice to achieve the best recovery performance. The selection of an optimum discharging rate should keep a balance between SOC inhomogeneity of the electrode material and the recovery time.

4.3. Bottom recovery on the commercial/novel battery with varying discharging current

The simulation results the for bottom recovery method with varying discharging current are shown in Figs. 9–11. The recovery

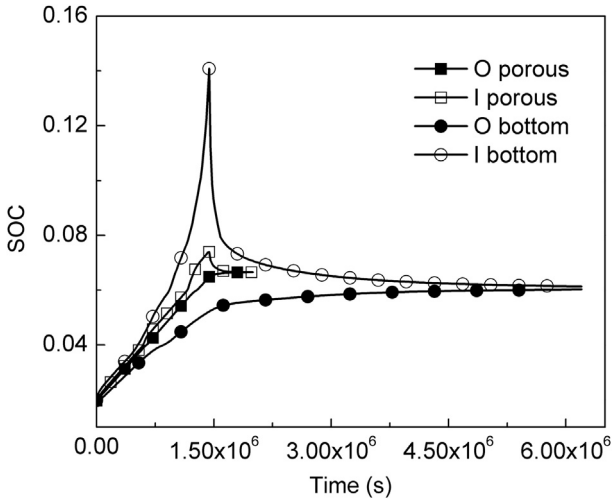

Fig. 12. Comparison of solid surface concentration evolution between bottom recovery and center recovery for novel battery with porous current collectors.

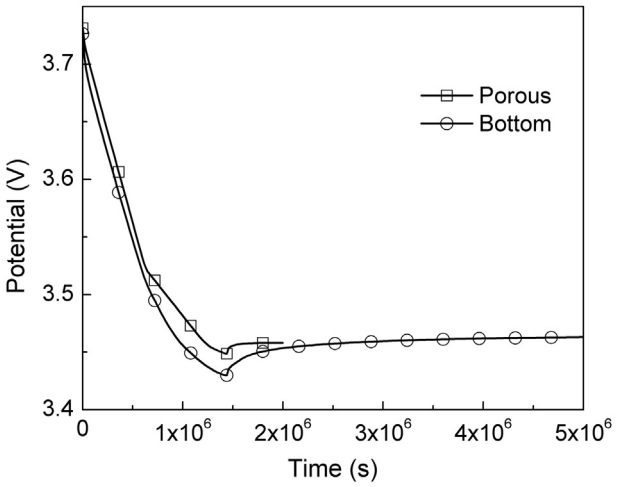

Fig. 14. Comparison of potential evolution between bottom recovery and center recovery for battery with porous current collector.

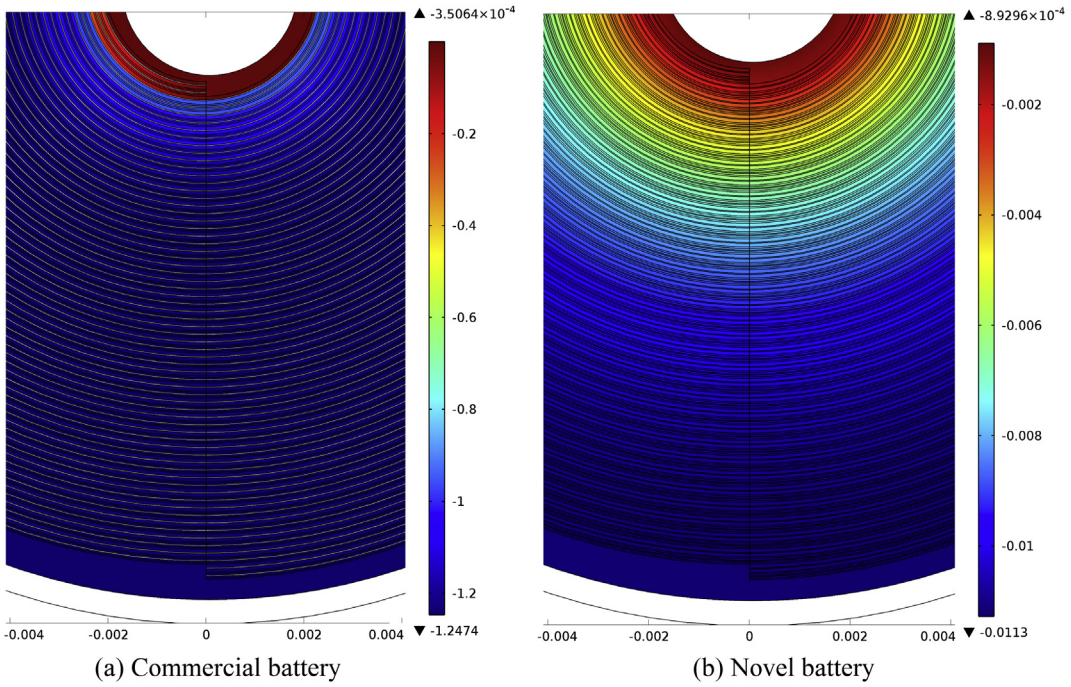

Fig. 15. Comparison of liquid potential between center recovery for battery with normal current collector and battery with porous current collector.

time for a 5 mA discharging current is 1/10 of that for a 0.5 mA discharging current (Fig. 9), but the total recovery time which includes the relaxation time is almost the same between 5 mA and 0.5 mA discharging currents. The solid surface concentration distribution follows the same trend as that for center recovery, that is, concentration gradient increases as the discharging current increases (Fig. 10).

The simulation is cut off when the maximum SOC of the electrode reaches 1, so the simulation for the 50 mA bottom recovery process is not complete, and as shown in Fig. 11, the discharging potential drop sharply to 2.5 V before the 200 mAh recovery is completed. When comparing the cases of 50 mA recovery between center recovery and bottom recovery, Figs. 6–11, we find that the center recovery method for novel batteries with porous current

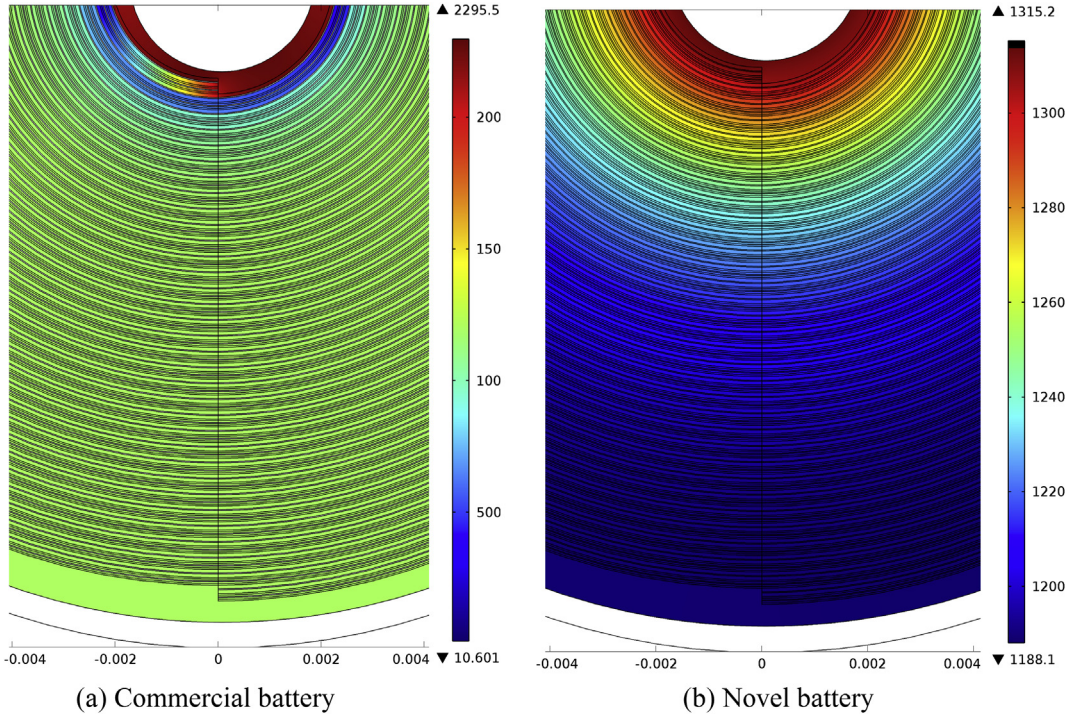

Fig. 16. Comparison of liquid concentration between center recovery for battery with normal current collector and battery with porous current collector.

collector sheets performs much better than the bottom recovery method. This conclusion may be further verified in the following detailed comparison between center recovery and bottom recovery (0.5 mA).

4.4. Comparison between center recovery and bottom recovery on the novel battery (at 0.5 mA current)

Comparisons of SOC evolution, SOC distribution, and discharging potential between the center recovery method for novel batteries with porous current collectors and the bottom recovery method are shown in Figs. 12–14, respectively. The results show that the center recovery method gives rise to moderate SOC gradients (Fig. 13), smaller maximum SOC (Fig. 12), and gradual potential drops (Fig. 14).

The relaxation time for center recovery for novel batteries is much less than that for bottom recovery. The solid surface lithium ion concentration is much more uniform in center recovery than that in bottom recovery. Potential drop for center recovery is also smaller than that for bottom recovery. We may conclude that center recovery is more effective than bottom recovery in terms of both SOC distribution and recovery time.

4.5. Analysis on lithium ion transport path

The phenomenon of different performance of different recovery methods on different batteries is presumably due to the difference in lithium ion transport paths. The liquid potential gradient and liquid phase concentration gradient are much larger in commercial batteries with normal current collector foils than those in novel batteries with porous current collector sheets as shown in Figs. 15 and16. The reason is that, the pores in the porous current collector sheet offer paths for liquid phase transportation and ionic conduction, which is straightforward to see from the electrolyte current density vectors shown in Fig. 17. Consequently, the distance for liquid transportation from the center of the battery to the battery casing is the radius of the battery, R. For the battery with normal current collector foils, the transport path is the passage sandwiched by two spiral-wound current collector foils, and the length of the transport path would then be the length of the current

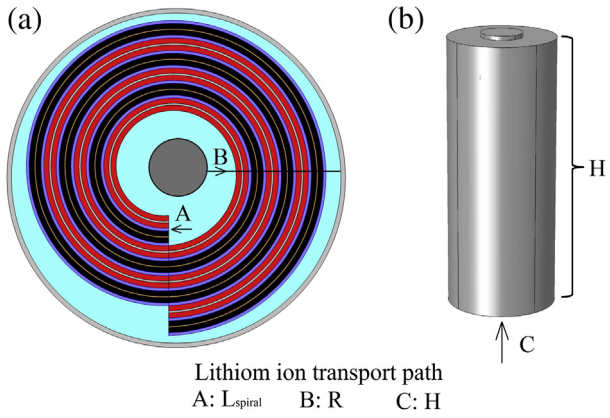

Fig. 18. Comparison of liquid path of battery with commercial battery and novel battery.

collector L_{spiral}. For a clear view of this transport path, readers can refer to the length of boundary B4 in Fig. 1.

For the bottom recovery method suggested by Wang et al. [1], the transport path for the liquid phase is also the space sandwiched between current collector foils, while the direction is from the bottom end to the top end of the battery. Therefore, the transport path is the height of the battery, H. Take the 26650 cylindrical battery for example, as shown in Fig. 18, we find that the transport path for liquid in the case of center recovery for a commercial battery with normal current collector foils is 1.45 m (L_{spiral}), that for center recovery for a novel battery with porous current collector sheets is 0.013 m (R), and that for bottom recovery is 0.065 m (H). The comparison of transport paths shows clearly why center recovery of batteries with normal current collector foils is impractical, and why center recovery of novel batteries with porous current collector sheets is superior to bottom recovery.

4.6. Comparison between positive electrode recovery and negative electrode recovery on the novel battery (center recovery at 5 mA)

Besides recovery by discharging the positive electrodes of the battery, recovery of capacity by discharging the negative electrodes

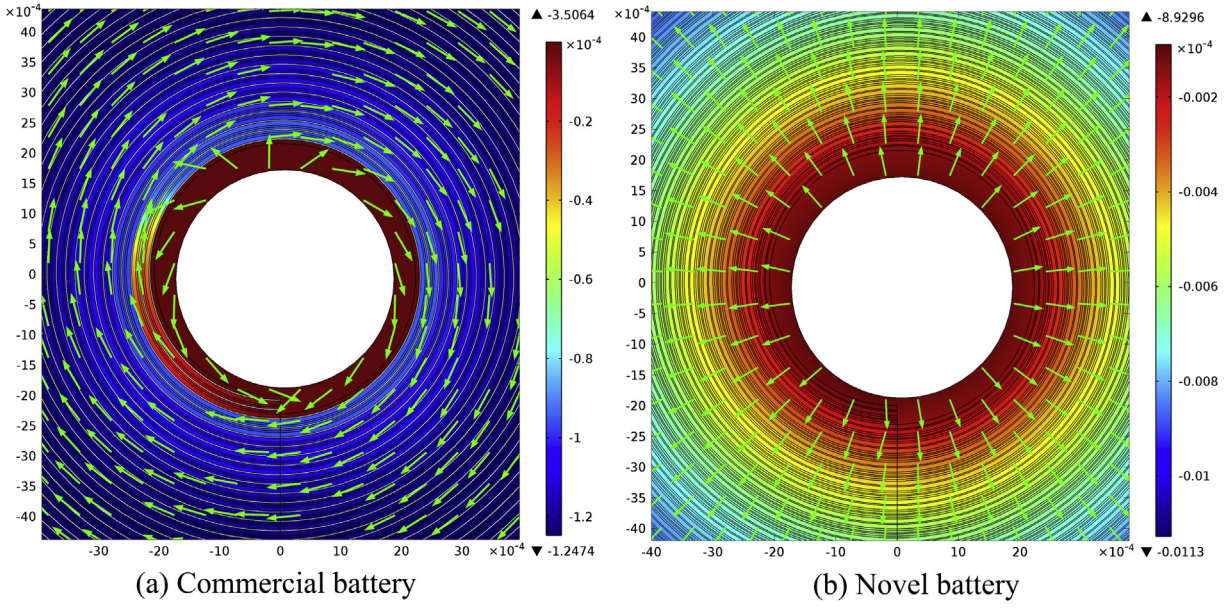

Fig. 17. Comparison of electrolyte current density vectors between center recovery for commercial battery and novel battery.

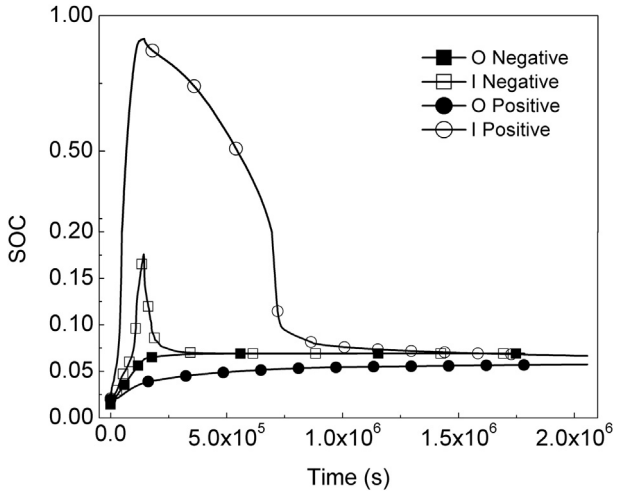

Fig. 19. Comparison of solid surface concentration for center recovery of novel battery between discharging the negative electrode and discharging the positive electrode.

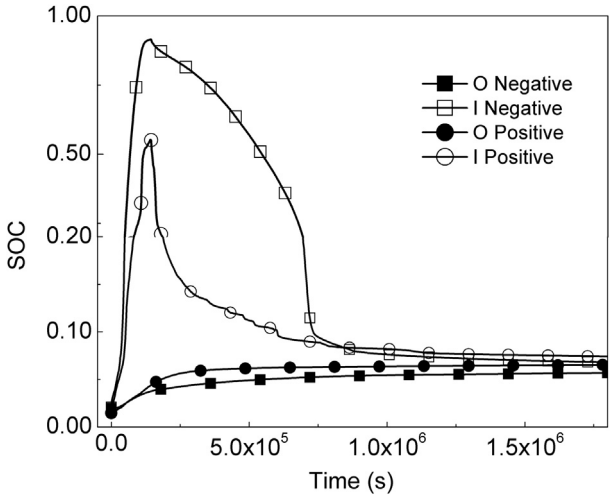

Fig. 20. Comparison of solid surface concentration evolution for bottom recovery between charging the negative electrode and charging the positive electrode.

of the battery was also suggested in our previous work [10]. It is also of interest to investigate the feasibility of the method and to compare its recovery capability with that of discharging the positive electrode.

For modeling the recovery process of discharging negative electrodes, a current source is applied on the negative current collectors. The simulation results for solid surface lithium ion concentrations are shown in Fig. 19.It is apparent that the concentration is more uniform than that for recovery with positive electrode discharging. The relaxation time is also much less and the battery reaches the equilibrium state much faster. Thus, capacity recovery by discharging the negative electrode is better than by discharging the positive electrode in terms of both SOC distribution and recovery time. The reason for this phenomenon appears to be due to the higher reaction rate and better lithium ion diffusion in the negative electrode than in the positive electrode. For the 26650 lithium iron phosphate battery in this study, the diffusivity of the negative electrode (3.9×10^{-14}) is much higher than that of the positive electrode (1.18×10^{-18}), leading to a higher local reaction rate constant of3×10^{-11} for the negative electrode compared to 1.4×10^{-12} for the positive electrode.

4.7. Comparison between positive electrode recovery and negative electrode recovery on the commercial/novel battery (bottom recovery at 5 mA)

Similar results are found in the case of bottom recovery between discharging positive electrodes and discharging negative electrodes (Fig. 20). Though there is no significant difference in the total recovery time, much larger maximum concentration is found in discharging the positive electrode than in discharging the negative electrode (SOC = 0.95 as compared to SOC = 0.5).

Capacity recovery by discharging the negative electrode shows better performance in lower maximum SOC and shorter total recovery time than recovery by discharging the positive electrode. One important aspect to point out is that, lithium deposition would occur at the negative electrode during overcharging [17], and it has been shown that negative electrodes (graphite or carbon) experience higher risk of lithium deposition during over discharging than positive electrodes [2,7]. Nevertheless, overcharging of positive electrodes may also cause solvent oxidation which accelerates capacity loss of the battery. So the recovery current should be carefully chosen to avoid high maximum SOC of the electrode material during the recovery process.

5. Conclusion

In this study, an electrochemical model for spiral wound lithium ion battery is developed for the study of capacity recovery methods for cycled batteries. Simulations are done to study the feasibility and effectiveness of the recovery method which is proposed in our previous study by discharging the positive electrode or negative electrode against a lithium metal electrode inserted into the center of the cycled battery.

Simulation results show that the center recovery method is not applicable for commercial batteries with normal current collector foils due to severe concentration gradients in the spiral geometry, and significant potential drops during recovery. However, the center recovery method shows much better performance on novel batteries with porous current collector sheets in terms of SOC uniformity and recovery time. The differences in performance between the different recovery methods are found to be mainly due to the differences in the lithium ion transport paths. The shorter the lithium ion transport path, the better the recovery performance.

The capacity recovery process can be realized either by discharging the positive electrode or by discharging the negative electrode. The simulation results in this study indicate that the performance after recovery by discharging the negative electrode is better than that by discharging the positive electrode in terms of both SOC uniformity and recovery time, due to higher lithium ion diffusivity in the negative electrode material.

References

[1] J. Wang, S. Soukiazian, M. Verbrugge, H. Tataria, D. Coates, D. Hall, P. Liu, J. Power Sources 196 (2011) 5966–5969.
[2] P. Arora, R.E. White, M. Doyle, J. Electrochem Soc. 145 (1998) 3647–3667.
[3] M. Broussely, P. Biensan, F. Bonhomme, P. Blanchard, S. Herreyre, K. Nechev, R.J. Staniewicz, J. Power Sources 146 (2005) 90–96.
[4] T. Yoshida, M. Takahashi, S. Morikawa, C. Ihara, H. Katsukawa, T. Shiratsuchi, J. Yamaki, J. Electrochem Soc. 153 (2006) A576–A582.
[5] M. Balasubramanian, H.S. Lee, X. Sun, X.Q. Yang, A.R. Moodenbaugh, J. McBreen, D.A. Fischer, Z. Fu, Electrochem Solid State-Lett. 5 (2002) A22–A25.
[6] R. Spotnitz, J. Power Sources 113 (2003) 72–80.
[7] P. Liu, J. Wang, J. Hicks-Garner, E. Sherman, S. Soukiazian, M. Verbrugge, H. Tataria, J. Musser, P. Finamore, J. Electrochem Soc. 157 (2010) A499–A507.

[8] P. Ramadass, B. Haran, P.M. Gomadam, R. White, B.N. Popov, J. Electrochem Soc. 151 (2004) A196–A203.
[9] J. Christensen, J. Newman, J. Electrochem Soc. 152 (2005) A818–A829.
[10] Y. Ye, Y. Shi, A.A.O. Tay, J. Power Sources 217 (2012) 509–518.
[11] Y.H. Ding, J.X. Li, Y. Zhao, L.H. Guan, Mater. Lett. 81 (2012) 105–107.
[12] W. Xu, N.L. Canfield, D.Y. Wang, J. Xiao, Z.M. Nie, X. Li, W.D. Bennett, C.C. Bonham, J.G. Zhang, J. Electrochem Soc. 157 (2010) A765–A769.
[13] K. Somasundaram, E. Birgersson, A.S. Mujumdar, J. Power Sources 203 (2012) 84–96.
[14] M. Doyle, T.F. Fuller, J. Newman, J. Electrochem Soc. 140 (1993) 1526–1533.
[15] D.A.G. Bruggeman, Ann. Phys-Berlin 416 (1935) 636–664.
[16] J. Wang, P. Liu, J. Hicks-Garner, E. Sherman, S. Soukiazian, M. Verbrugge, H. Tataria, J. Musser, P. Finamore, J. Power Sources 196 (2011) 3942–3948.
[17] P. Arora, M. Doyle, R.E. White, J. Electrochem Soc. 146 (1999) 3543–3553.